Supplemental Material

Text 1. Analysis methods

Text 2. Effects of alteration and low–grade metamorphism

Table S1. Zircon U–Pb analytical data of Yingen and Quagu plutons in the southern Alxa.

Table S2. Zircon Hf isotopic compositions of Yingen and Quagu plutons in the southern Alxa.

Table S3. Major and trace elements compositions of Yingen and Quagu plutons in the southern Alxa.

Table S4. Whole rock Rb-Sr and Sm-Nd isotopic compositions of Yingen and Quagu plutons in the southern Alxa.

Table S5. Summary of zircon U-Pb age and Hf isotope data of ophiolites and plutons in the southern Alxa.

1. ANALYSIS METHODS

In this study, we analyzed zircon U–Pb ages, whole-rock major and trace element, and in situ Lu–Hf isotopes in zircons for Yingen and Quagu plutons in the southern Alxa. Detailed analysis methods are presented below.

1.1 Zircon U-Pb dating analysis

1.1.1 Zircon LA-ICP-MS U–Pb dating

Zircons from crushed samples were separated by using conventional heavy liquid and magnetic techniques in the Laboratory of Langfang Regional Geological Survey, Hebei Province, China. Representative zircon grains were hand-picked under a binocular microscope, mounted in epoxy resin, polished, and coated with gold film. Zircons were photographed in transmitted and reflected light. Those photos, together with cathodoluminescence (CL) images were used to examine the external and internal structures of the analyzed zircons at the Gaonian Navigation Technology Company, Beijing, China.

Laser ablation (LA)–ICP MS zircon U-Pb geochronological dating was carried out at Beijing Createch Testing Technology Co.,Ltd. Detailed operating conditions for the laser ablation system and the ICP-MS instrument and data reduction are the same as description by Hou et al. (2009). Laser sampling was performed using a RESOlution 193 nm laser ablation system. An Agilent 7500 ICP-MS instrument was used to acquire ion-signal intensities. Helium was applied as a carrier gas. Argon was used as the make-up gas and mixed with the carrier gas via a T-connector before entering the ICP. Each analysis incorporated a background acquisition of ~15–20 s (gas blank) followed by 45 s data acquisition from the sample. Off-line raw data selection and integration of background and analyte signals, and time-drift correction and quantitative calibration for U-Pb dating was performed by *ICPMSDataCal* (Liu et al., 2010). Zircon GJ-1 was used as external standard for U-Pb dating, and was analyzed twice every 5–10 analyses. Time-dependent drifts of U-Th-Pb isotopic ratios were corrected using a linear interpolation (with time) for every 5–10 analyses according to the variations of GJ-1 (i.e., 2 zircon GJ-1 + 5–10 samples + 2 zircon GJ-1) (Liu et al., 2010). Uncertainty of preferred values for the external standard GJ-1 was propagated to the ultimate results of the samples. In all analyzed zircon grains the common Pb correction was not necessary due to the low signal of common ^{204}Pb and high ^{206}Pb/^{204}Pb. U, Th and Pb concentration was calibrated by NIST 610. Concordia diagrams and weighted mean calculations were made using Isoplot/Ex_ver3. The zircon Plesovice is dated as unkown samples and yielded weighted mean ^{206}Pb/^{238}U age of 337.8 ± 2.3 Ma (2SD, n = 40), which is in good agreement with the recommended ^{206}Pb/^{238}U age of 337.13 ± 0.37 Ma (2SD) (Sláma et al., 2008). The U-Pb data are listed in the Appendix Table S1.

1.1.2 Zircon SHRIMP U-Pb analyses

Separation of zircon crystals was accomplished by conventional heavy liquid and magnetic techniques. The individual crystals were mounted in epoxy together with the TEMORA standard zircons, and then polished to approximately half their original thickness. Zircon grains were then photographed by optical microscopy, and cathodoluminescence (CL) images were obtained using a HITACHI S-3000N SEM with accelerating voltage of 10 kV and an electron current of 100 μA. U-Pb isotopic ratios of zircon crystals from the sample of 19AL01–2 were measured using the SHRIMP II in the Beijing SHRIMP Center, Institute of Geology, Chinese Academy of Geological Sciences, Beijing, China. Instrumental conditions and

measurement procedures are the same as those described by Compston et al. (1992). Spots of ~20μm-diameter were analyzed. Data for each spot were collected in sets of five scans. The $^{206}Pb/^{238}U$ ratios of the samples were corrected using reference zircon of TEMORA ($^{206}Pb/^{238}U$ = 0.06683; 417 Ma), and U concentrations were normalized using reference zircon of M257 (U = 840 ppm, Nasdala et al., 2008). The data were corrected for common Pb on the basis of the measured ^{204}Pb. The decay constants and present-day $^{238}U/^{235}U$ value given by Steiger and Jager (1977) were used. Data processing and assessment was carried out using the SQUID and ISOPLOT programs (Ludwig, 2003). Uncertainties for the isotopic ratios of individual analyses in Appendix Table S1 and on the concordia diagrams are given at 1σ, whereas uncertainties for weighted mean ages in the text are quoted at the 95% confidence level. The SHRIMP U-Pb data are listed in the Appendix Table S1.

1.2. Major and trace elemental analyses

Whole-rock major and trace element compositions were analyzed at Beijing Createch Testing Technology Co.,Ltd., China. Major element compositions were determined by XRF (Shimadzu XRF-1800); the analytical precision was within 1%. The trace element compositions analysis was conducted by following the technique of Li (1997). Approximately 25 mg of each sample was dissolved in high-pressure Teflon beakers by using a $HF+HNO_3$ mixture. The solutions were centrifuged after dissolution, and the supernatants were moved to clean Teflon beakers. The solutions were evaporated to near dryness and then added 1.0 ml concentrated HNO_3 and dried twice to eliminate the influence of the HF or HCl. Afterward, all the analyzed samples were dissolved in 2% HNO_3 solution with an internal standard Rh for analysis. The trace element compositions were analyzed by using a Analyticjena PQMS elite inductively coupled plasma mass spectrometer (ICP-MS) and the analytical uncertainties were mostly better than 5%.

1.3. In Situ zircon Hf isotopic analyses

Zircon in situ Hf isotope analysis was carried out using a RESOlution SE 193nm laser-ablation system attached to a Thermo Fisher Scientific Neptune Plus MC-ICP-MS at Beijing Createch Testing Technology Co., Ltd. Instrumental conditions and data acquisition protocols were described by Hou et al. (2007). A stationary spot used a beam diameter of ~38 μm. As the carrier gas, helium was used to transport the ablated sample aerosol mixed with Argon from the laser-ablation cell to the MC-ICP-MS torch by a mixing chamber. $^{176}Lu/^{175}Lu$ = 0.02658 and $^{176}Yb/^{173}Yb$ = 0.796218 ratios were determined to correct for the isobaric interferences of ^{176}Lu and ^{176}Yb on ^{176}Hf. For instrumental mass bias correction Yb isotope ratios were normalized to $^{172}Yb/^{173}Yb$ = 1.35274 and Hf isotope ratios to $^{179}Hf/^{177}Hf$ = 0.7325 using an exponential law. The mass bias behavior of Lu was assumed to follow that of Yb, the mass bias correction protocol was described by Hou et al. (2007). Zircon international standard GJ-1 was used as the reference standard.

1.4. Whole-rock Sr-Nd isotope analyses

Sr and Nd isotope analyses were measured in Beijing Createch Testing Technology Co., Ltd. All chemical preparations were conducted on class 100 work benches within a 1000 clean laboratory. About 150 mg of sample powder was weighted into a 15mL SavillexTM PFA screw-top beaker. Concentrated HNO3 and HF (1 mL and 2 mL) were added to the samples and the sealed beakers were heated on a hotplate at 150℃ for 1 week. After digestion, acids were evaporated on the hotplate and residues were dissolved in 1 mL of concentrated HCl. This procedure was then repeated 3 times. Finally, the samples were dissolved in 1.5 mL of 3.5 M HNO3 or 3 M HCl for Sr or Nd purification, respectively.

Sr was separated and purified from samples using Sr-Spec (Triskem, 100-150 μm) resin. For Nd purification, REEs (Rare Earth Elements) were first rinsed by 6 M HCl using the cation exchange resin (AG50W-X12, 200-400 mesh). Then Nd was purified from REEs by 0.25 M with LN resin (Triskem, 100-150 μm).

Isotopic compositions of Sr and Nd analyses were undertaken using a Thermo Fisher Scientific Neptune Plus MC-ICP-MS. $^{87}Sr/^{86}Sr$ ratios were corrected for instrumental mass fractionation using the exponential fractionation law and assuming $^{88}Sr/^{86}Sr = 8.375209$. $^{143}Nd/^{144}Nd$ ratios were corrected for instrumental mass fractionation using the exponential fractionation law and assuming $^{146}Nd/^{144}Nd = 0.7219$. The methods were modified from Yang et al.(2010). The BNVO-2 and BCR-2 standards measured during the analytical course gave $^{143}Nd/^{144}Nd$ of 0.512940 ± 6 (2σ) and 0.512626 ± 14 (2σ) values, and have $^{187}Sr/^{86}Sr$ of 0.703499 ± 6 (2σ) and 0.705027 ± 7 (2σ) values, respectively. $^{87}Rb/^{86}Sr$ and $^{147}Sm/^{144}Nd$ ratios are calculated using the Rb, Sr, Sm and Nd abundances measured by ICP-MS. The measured and age-corrected $^{87}Sr/^{86}Sr$ and $\varepsilon_{Nd}(t)$ are listed in Appendix Table S4.

REFERENCES CITED

Compston, W., Williams, I.S., Kirschvink, J.L., Zhang, Z., and Ma, G., 1992, Zircon U–Pb ages for the Early Cambrian timescale: Journal of the Geological Society, v. 149, p. 171–184, https://doi.org/10.1144/gsjgs.149.2.0171.

Hou, K.J., Li, Y.H., Zou, T.R., Qu, X.M., Shi, Y.R., and Xie, G.Q., 2007, Laser ablation-MC-ICP-MS technique for Hf isotope microanalysis of zircon and its geological applications. (in Chinese with English abstract): Yanshi Xuebao, v. 23, p. 2595–2604.

Hou K J, Li Y H, Tian Y Y. 2009. *In situ* U-Pb zircon dating using laser ablation-multi ion couting-ICP-MS. Mineral Deposits, 28(4):481-492. (in Chinese with English abstract)

Li, X.H., 1997, Geochemistry of the Longsheng ophiolite from the southern margin of Yangtze Craton, SE China: Journal of Geochemistry, v. 31, p. 323–337. https://doi.org/10.2343/geochemj.31.323

Liu, Y.S., Hu, Z.C., Zong, K.Q., et al., 2010, Reappraisement and refinement of zircon U-Pb isotope and trace element analyses by LA-ICP-MS: Chinese Science Bulletin, v. 55, no. 15, p. 1535–1546, https://doi.org/10.1007/s11434-010-3052-4.

Ludwig, K.R., 2003, Manual for Isoplot 3.7: Berkeley Geochronological Center Special Publication, v. 4, 77 p.

Nasdala, L., Miletich, R., Ruschel, K., and Váczi, T., 2008, Raman study of radiation-damaged zircon under hydrostatic compression: Physics and Chemistry of Minerals, v. 35, no. 10, p. 597–602, https://doi.org/10.1007/s00269-008-0251-5.

Sláma, J., Košler, J., Condon, D.J., Crowley, J.L., Gerdes, A., Hanchar, J.M., et al., 2008, Plešovice zircon—A new natural reference material for U–Pb and Hf isotopic microanalysis: Chemical Geology, v. 249, no. 1–2, p. 1–35, https://doi.org/10.1016/j.chemgeo.2007.11.005 .

Steiger, R.H., and Jager, E., 1977, Subcommission on geochronology: convention on the use of decay constants in geo-and cosmochronology: Earth and Planetary Science Letters, v. 36, no. 3, p. 359–362, https://doi.org/10.1016/0012-821X(77)90060-7.

Yang Y., Zhang H., Chu Z., Xie L. and Wu F., 2010, Combined chemical separation of Lu, Hf, Rb, Sr, Sm and Nd from a single rock digest and precise and accurate isotope determinations of Lu–Hf, Rb–Sr and Sm–Nd isotope systems using Multi-Collector ICP-MS and TIMS: International Journal of Mass Spectrometry, v. 290, p. 120–126. http://377.rm.cglhub.com/10.1016/j.ijms.2009.12.011

2. EFFECTS OF ALTERATION AND LOW–GRADE METAMORPHISM

All those analyzed samples in this study, including dikes within Yingen pluton, hosting granites, and Quagu diorites, exhibit low loss on ignition (LOI = 0.31–1.34 wt.%), which indicate insignificant effect of alteration and low–grade metamorphism in the post–magmatic processes. Besides, all the samples have consistent and coherent primitive mantle-normalized trace element patterns (Fig. 8), which also support the insignificant effect. Moreover, previous studies show that Zr is one of the least mobile elements in low–grade metamorphism and alteration process (e.g., Polat et al., 2002 and references therein), thus Zr is used as an alteration-independent index of geochemical variations (Pearce et al., 1992), and correlations between other elements and Zr can be used to evaluate the mobility of elements during post–magmatic processes (e.g., Polat et al., 2002; Polat and Hofmann, 2003). Mobilities of elements selected in the discussion are confirmed in the supplemental Figure S1. The high field strength elements (HFSE, such as Nb), REEs (), Sr, Th, and Y are strongly correlated with Zr, indicating that these elements were essentially immobile during metamorphism and alteration (Polat et al., 2002). Therefore, the low–grade metamorphism is considered to have had an insignificant effect on mobilities of those elements.
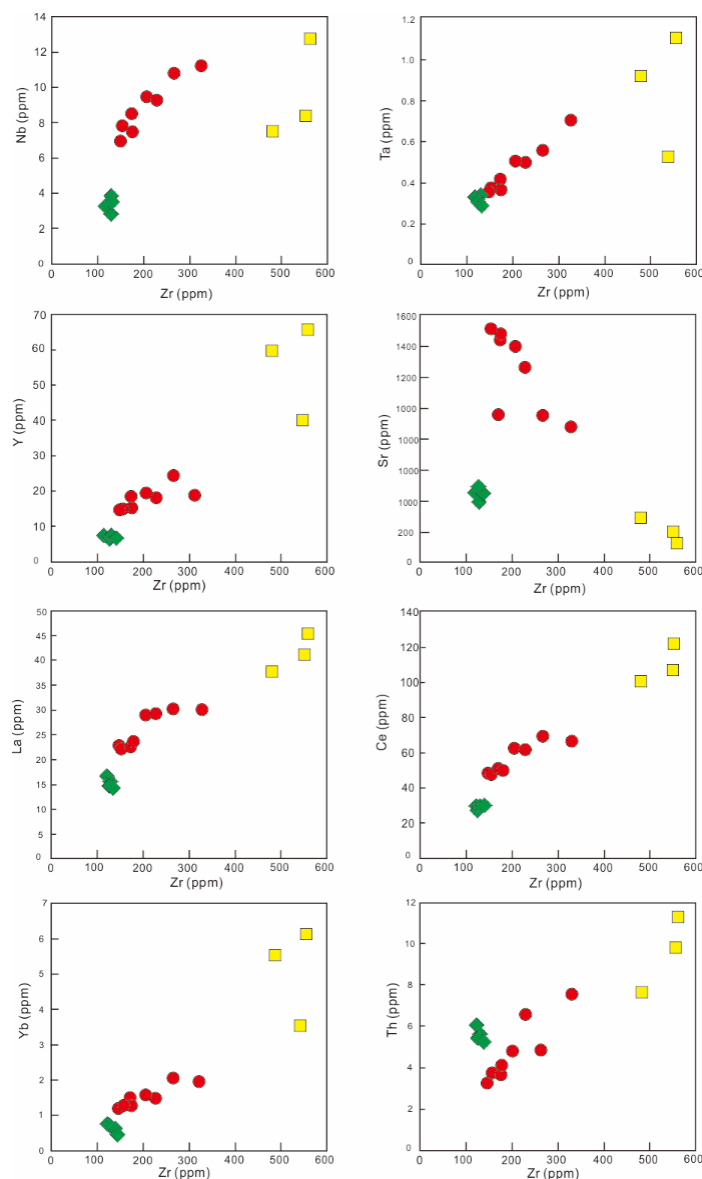
Figure S1. Elements versus Zr correlation diagrams for Yingen and Quagu plutons

REFERENCES CITED

Pearce, J.A., van der Laan, S., Arculus, R.J., Murton, B.J., Ishii, T., and Peate, D.W., 1992, Boninite and Harzburgite from Leg 125 (Bonin– Mariana Fore-arc): a case study of magma genesis during the initial stage of subduction, *in* Fryer, P., Pearce, J.A., and Stokking, L.B., eds., Proceedings for the ocean drilling program, Scientific Results, v. 125, p. 623–659.

Polat, A., and Hofmann, A., 2003, Alteration and geochemical patterns in the 3.7–3.8 Ga Isua greenstone belt, West Greenland: Precambrian Research, v. 126, no. 3–4, p. 197–218, https://doi.org/10.1016/S0301-9268(03)00095-0.

Polat, A., Hofmann, A., and Rosing, M.T., 2002, Boninite-like volcanic rocks in the 3.7–3.8 Ga Isua greenstone belt, West Greenland: geochemical evidence for intra-oceanic subduction zone processes in the early Earth: Chemical Geology, v. 184, no. 3–4, p. 231–254, https://doi.org/10.1016/S0009-2541(01)00363-1.